nature physics

LETTERS

https://doi.org/10.1038/s41567-021-01226-y

Check for updates

Absolute $^{13}C/^{12}C$ isotope amount ratio for Vienna PeeDee Belemnite from infrared absorption spectroscopy

Adam J. Fleisher[1,5]✉, Hongming Yi[1,4,5], Abneesh Srivastava[1], Oleg L. Polyansky[2,3], Nikolai F. Zobov[3] and Joseph T. Hodges[1]

Measurements of isotope ratios are predominantly made with reference to standard specimens that have been characterized in the past. In the 1950s, the carbon isotope ratio was referenced to a belemnite sample collected by Heinz Lowenstam and Harold Urey[1] in South Carolina's PeeDee region. Due to exhaustion of the sample since then, reference materials that are traceable to the original artefact are used to define the Vienna PeeDee Belemnite scale for stable carbon isotope analysis[2]. However, these reference materials have also become exhausted or proven to exhibit unstable composition over time[3], mirroring issues with the international prototype of the kilogram that led to a revised International System of Units[4]. A campaign to elucidate the stable carbon isotope ratio of Vienna PeeDee Belemnite is underway[5], but independent measurement techniques are required to support it. Here we report an accurate value for the stable carbon isotope ratio inferred from infrared absorption spectroscopy, fulfilling the promise of this fundamentally accurate approach[6]. Our results agree with a value recently derived from mass spectrometry[5] and therefore advance the prospects of International System of Units–traceable isotope analysis. Further, our calibration-free method could improve mass balance calculations and enhance isotopic tracer studies in carbon dioxide source apportionment.

Small variations in the isotopic abundances of common nuclei such as carbon, oxygen and hydrogen occur naturally. The isotope delta notation is a useful expression for precision stable isotope analysis and is generally defined as $\delta^iE = R(^iE/^jE)_{sample}/R(^iE/^jE)_{ref} - 1$, where i is the heavier isotope mass number of element E (for example, ^{13}C); j is the lighter isotope mass number of E (for example, ^{12}C); and $R(^iE/^jE)_{sample}$ and $R(^iE/^jE)_{ref}$ are the absolute isotope ratios of an unknown sample and a reference material, respectively (for example, $R(^{13}C/^{12}C)_{sample}$ and $R(^{13}C/^{12}C)_{ref}$) (ref. [7]). The δ notation—expressed per mille using the symbol ‰, where $1‰ \equiv 1 \times 10^{-3}$—allows for the convenient expression of exceedingly small differences in isotope composition and thus an accessible discussion of subjects as diverse as variability in atmospheric composition, climatology, geochemistry, ecology, and dietary evolution and networking.

To measure small differences on a δ scale, ultraprecise analytical techniques such as isotope ratio mass spectrometry (IRMS)[8] and Fourier transform infrared spectroscopy[9], based on the identical treatment of sample and reference, are commonly used. Although δ values can be determined with a precision of ≤0.01‰, absolute isotope ratio measurements of $R(^iE/^jE)_{sample}$ with commensurate accuracy have not been possible because of either systematic uncertainties in the values of $R(^iE/^jE)_{ref}$ or the achievable uncertainty in primary methods such as calibration using synthetic isotope mixtures. For example, the most recent evaluation of the Vienna PeeDee Belemnite (VPDB) reference ratio that underpins the $\delta^{13}C$ scale, namely, $R(^{13}C/^{12}C)_{VPDB}$, reported uncertainties that were more than 100-fold greater than the achievable δ-value precision[5]. The lack of independent experimental techniques for stable carbon isotope ratio measurements has generally impeded the assessment of uncertainty in $R(^{13}C/^{12}C)_{ref}$ values and confounded efforts to correct for their respective drifts over time[3].

The δ notation has additional limits. For example, δ values are approximately a linear function of mole fraction only for very small differences between $R(^iE/^jE)_{sample}$ and $R(^iE/^jE)_{ref}$, and multiple reference materials are required to establish linearity[2]. For samples with large differences between $R(^iE/^jE)_{sample}$ and $R(^iE/^jE)_{ref}$ (for example, samples enriched or depleted in ^{13}C, or extraterrestrial samples), δ values are a highly nonlinear function of the mole fraction[7], and precision is generally degraded when measuring sample values far from the scale definition ($\delta^iE = 0$). For several applications, direct measurements of $R(^iE/^jE)_{sample}$ or atom (mole) fraction would be advantageous. These include tracer studies for enriched compound- or position-specific isotope analysis[10] and the calculation of mixing ratios in complex systems using a mass balance equation (for example, systems with two or more sources and/or sinks of variable isotopic composition[7]). From a standards and metrology perspective, direct measurements of $R(^iE/^jE)_{sample}$ would enable detailed studies of drifts in primary reference materials[3] and International System of Units (SI)-traceable isotope ratio determinations[5]. Accurate measurements of $R(^iE/^jE)_{sample}$ that are traceable to intrinsic physical invariants would also maintain compatibility with historical δ notation scales by underpinning the isotope ratios of primary and secondary reference materials. This is highly desirable, given that the ratio-of-ratios approach conveniently expressed by the δ notation is inherently susceptible to temporal instability and physical inhomogeneity in the required traceability chain and two-point calibration schemes. Finally, reliable scales that eliminate artefacts altogether are desirable when measuring isotope ratios in extreme environments like those encountered during Solar System exploration. In these cases, carrying bulky and consumable specimens can

[1]Material Measurement Laboratory, National Institute of Standards and Technology, Gaithersburg, MD, USA. [2]Department of Physics and Astronomy, University College London, London, UK. [3]Institute of Applied Physics, Russian Academy of Sciences, Nizhny Novgorod, Russia. [4]Present address: Department of Civil and Environmental Engineering, Princeton University, Princeton, NJ, USA. [5]These authors contributed equally: Adam J. Fleisher, Hongming Yi. ✉e-mail: adam.fleisher@nist.gov

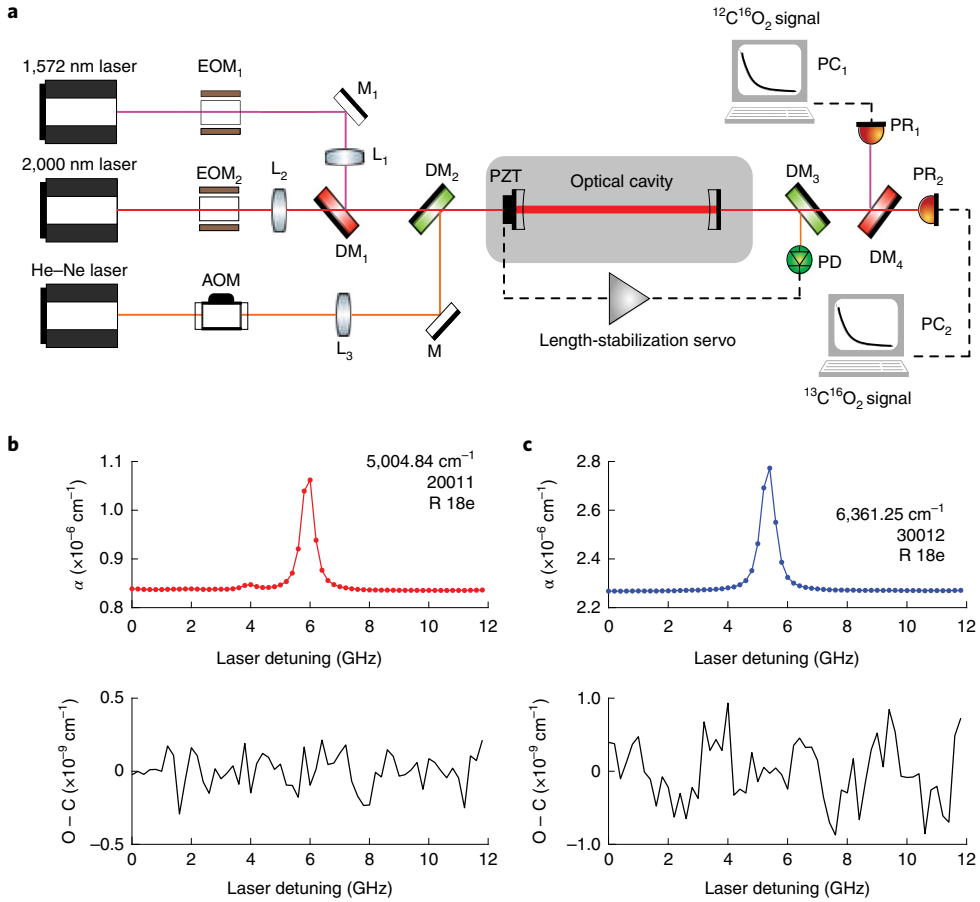

Fig. 1 | AIR-IS. a, The spectrometer synchronously probed two infrared transitions using diode lasers at wavelengths nominally equal to 2.0 μm ($^{13}C^{16}O_2$) and 1.6 μm ($^{12}C^{16}O_2$). Frequency-agile rapid scanning was accomplished via two electro-optic modulators (EOMs) driven by individual radiofrequency function generators. The length-stabilized optical enhancement cavity and sample cell provided effective path lengths of 12.0 km and 4.5 km at 2.0 μm and 1.6 μm, respectively. Laser light transmitted by the cavity was split at a dichroic mirror (DM) and then directed onto one of the two photoreceivers (PRs). AOM, acousto-optic modulator; M, reflective mirror; L, lens; PZT, piezo-electric transducer; PD, photodetector; PC, personal computer. **b**,**c**, Representative high-resolution cavity ring-down absorption spectra of $^{13}C^{16}O_2$ (**b**) and $^{12}C^{16}O_2$ (**c**) for a sample of NIST Standard Reference Material 1720 Northern Continental Air (χ_{CO_2} = 393.23 μmol mol^{-1}; $\delta^{13}C$ = –8.6‰). Measured absorption coefficients (α) in units of inverse length are plotted in the upper panels as a function of laser detuning (**b**, red dots, 2.0 μm laser; **c**, blue dots, 1.6 μm laser). Individual fitted spectral models (solid lines) are also shown, and the known transition frequency, vibrational band assignments and rotational transition assignments are listed (Supplementary Section 1). The lower panels show the observed-minus-calculated (O – C) fit residuals for each measured CO_2 transition.

be cost-prohibitive and pre-launch calibration routines are necessary to validate measurements like the isotopic composition of the modern Martian atmosphere[11].

Optical methods to directly measure $R(^iE/^jE)_{sample}$—circumventing the δ notation—have been proposed for decades[6]. Several notable efforts were focused on improving measurement precision and infrared transitions were studied over a narrow wavelength range[12–15]. That approach is problematic even when the absorption cross-sections—intrinsic molecular quantities that scale the isotope amounts—are well known[16]. Transitions involving different isotopic substitutions of the same molecule that occur at wavelengths near to one another often originate from very different rotational states, and consequently, substantial temperature biases are introduced. Those biases can be mitigated through a high degree of temperature control[17,18] or by studying pairs of transitions with nearly identical lower-state rotational energy[19]. While these prior proposals and proof-of-principle demonstrations collectively suggest that accurate optical measurements of $R(^iE/^jE)_{sample}$ may be possible without calibrations, each prior work was limited by either the aforementioned temperature biases or by uncertainties in the chosen absorption cross-sections. As a result, the absolute isotope ratios of reference materials inferred from accurate infrared absorption spectroscopy measurements have never been compared with SI-traceable mass spectrometry values.

Here we overcome both experimental hurdles using accurately known absorption cross-sections for carbon dioxide (CO_2) transitions from two distinct wavelength regions—effectively eliminating temperature biases. The results are direct measurements of $R(^iE/^jE)_{sample}$ by infrared absorption spectroscopy with an uncertainty commensurate with calibrated mass spectrometry. By also performing state-of-the-art IRMS on our CO_2-in-air gas samples, we infer $R(^{13}C/^{12}C)_{VPDB} = 0.011125 \pm 0.000043$. The value of $R(^{13}C/^{12}C)_{VPDB}$ derived from our unified measurement approach is in excellent agreement with other recently reported values[5] and differs significantly from the historic value of Craig[20]. Consequently, our results demonstrate the potential for perpetual and direct SI traceability in stable carbon isotope analysis, thus circumventing limitations associated with curation and further propagation of the new physical artefact standards that underpin the $\delta^{13}C$ VPDB scale[21].

Our accurate isotope ratio infrared spectroscopy (AIR-IS) instrument, illustrated in Fig. 1a, is a robust platform for measuring the mole fraction of both $^{13}CO_2$ and $^{12}CO_2$ and therefore the stable carbon

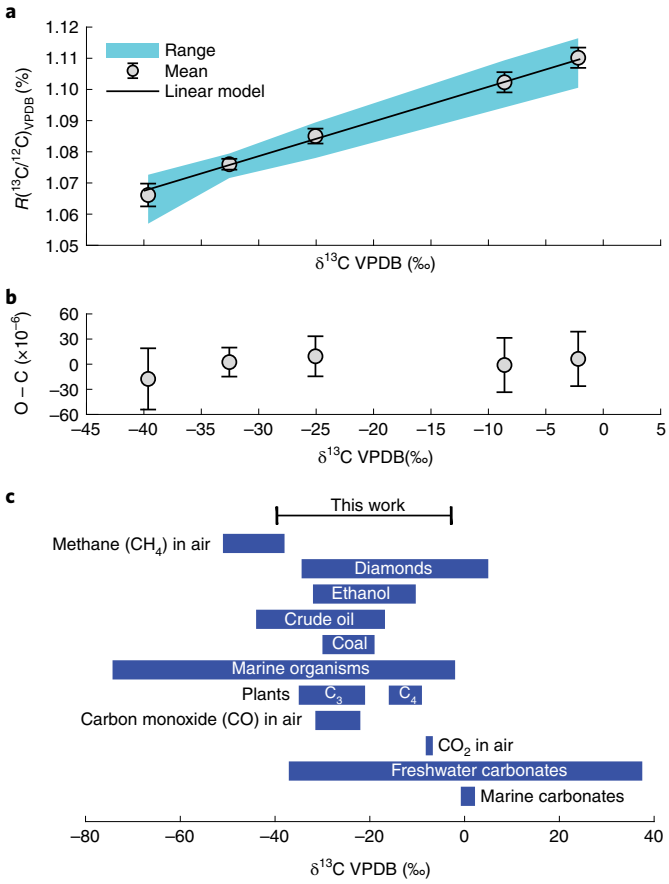

Fig. 2 | AIR-IS measurements of $R(^{13}C/^{12}C)_{sample}$ versus IRMS assignments of $\delta^{13}C$. a, AIR-IS values of $R(^{13}C/^{12}C)_{sample}$ were measured for five CO_2-in-air samples with $\delta^{13}C$ VPDB value assignments by IRMS. The light-blue shaded region is the interpolated area bounded by the range of measured $R(^{13}C/^{12}C)_{sample}$ values, while the mean and standard deviation for all five samples are plotted as grey circles. The black line represents a linear regression using the expression $R(^{13}C/^{12}C)_{sample} = R(^{13}C/^{12}C)_{VPDB} \times ((\delta^{13}C) + 1)$. **b**, Fitted residuals (O – C), along with their corresponding standard deviations. **c**, Expanded range of $\delta^{13}C$ values for some terrestrial and marine carbon sources[23].

isotope ratio of a gas sample. Typical relative measurement precision of $R(^{13}C/^{12}C)_{sample}$ for a 3 min spectral acquisition was 0.2×10^{-3}, with a best recorded relative precision of 0.13×10^{-3} (comparable to the World Meteorological Organization (WMO)/International Atomic Energy Agency extended compatibility goal for $\delta^{13}C$ of ±0.1‰ (ref. [22])). We simultaneously probed $^{13}CO_2$ and $^{12}CO_2$ rotational–vibrational transition pairs with nearly identical lower-state quantum numbers and lower-state energies and therefore effectively identical Boltzmann population factors (Supplementary Sections 1 and 3). Using diode lasers centred near wavelengths of 2.0 µm ($^{13}CO_2$) and 1.6 µm ($^{12}CO_2$) and high-reflectivity mirrors to form a single sample cell, the AIR-IS instrument created overlapping intra-cavity mode volumes for both wavelengths. This arrangement—combined with synchronous acquisition of the spectra—largely eliminated the influence of spatial–temporal temperature and pressure variations on the measured peak area ratios.

The absorption spectra of $^{13}C^{16}O_2$ and $^{12}C^{16}O_2$ in air at mole fractions within the range of natural terrestrial and marine abundances are shown in Fig. 1b,c. These spectra were measured using cavity ring-down spectroscopy and correspond to a reference sample of North American continental air with a value of $\delta^{13}C = -8.6$‰ realized by the WMO Global Atmosphere Watch Central Calibration Laboratory at the National Oceanic and Atmospheric Administration (NOAA). We report similar peak absorption coefficients for both isotopologues and thus similarly precise fits of the individual mole fractions $\chi = \frac{k_B T}{cS(T)p} \int \alpha(\nu)\, d\nu$, where c is the speed of light in a vacuum, k_B is the Boltzmann constant, T is the sample temperature, p is the total sample pressure, $S(T)$ is the unweighted temperature-dependent transition intensity (that is, not weighted by natural terrestrial isotopic relative abundances) and $\alpha(\nu)$ is the measured absorption coefficient as a function of frequency ν. Assuming that all stable isotopes of C (^{13}C and ^{12}C) and O (^{18}O, ^{17}O and ^{16}O) are randomly distributed amongst the corresponding isotopologues of CO_2, then $R(^{13}C/^{12}C)_{sample} = \chi(^{13}C^{16}O_2)/\chi(^{12}C^{16}O_2)$. Taking the ratio of the measured mole fractions of the two CO_2 isotopologues leads to the following working equation:

$$R\left(^{13}C/^{12}C\right)_{sample} = \frac{a_r}{s_r}, \quad (1)$$

where the subscript r indicates the $(^{13}C^{16}O_2)/(^{12}C^{16}O_2)$ ratio of parameters, $a \equiv \int \alpha(\nu)\, d\nu$ are the measured peak areas for each line and s_r is the line-intensity ratio for the transition pair. By concurrent measurements of a for both $^{13}C^{16}O_2$ and $^{12}C^{16}O_2$ at similar signal-to-noise ratios, we also eliminated biases associated with the relative frequency axis as well as with the choice of the lineshape profile.

Substituting equation (1) into the definition $\delta^{13}C = R(^{13}C/^{12}C)_{sample}/R(^{13}C/^{12}C)_{VPDB} - 1$ and solving for $R(^{13}C/^{12}C)_{VPDB}$ gives the VPDB reference value as follows:

$$R\left(^{13}C/^{12}C\right)_{VPDB} = \frac{a_r/s_r}{1 + \delta^{13}C}, \quad (2)$$

where all quantities on the right-hand side are based on values with quantifiable uncertainties.

We emphasize that the line intensities used to evaluate $R(^{13}C/^{12}C)_{sample}$ in equation (1) depend upon invariant molecular constants and a temperature-dependent function describing Boltzmann population statistics (Supplementary Section 3). As already stated, the temperature dependence of $s_r(T)$ was effectively eliminated by the choice of $^{13}C^{16}O_2$ and $^{12}C^{16}O_2$ transition pairs (Supplementary Section 1). For $^{13}C^{16}O_2$, we used intensities calculated here from an updated, fully ab initio dipole moment surface (DMS) and a semi-empirical potential energy surface (PES). This choice was justified by benchmarking the underlying quantum chemistry theory against accurate experiments (Supplementary Section 2).

AIR-IS measurements of $R(^{13}C/^{12}C)_{sample}$ for five CO_2-in-air samples are plotted in Fig. 2a versus $\delta^{13}C$ values assigned by IRMS (Supplementary Section 4). In Fig. 2a, the fitted black line reveals a high degree of linearity between the two techniques ($r^2 = 0.997$), and fitted residuals are plotted in Fig. 2b. Note that the CO_2-in-air samples were chosen to cover a broad range of $\delta^{13}C$ values that naturally occur across a wide variety of terrestrial and marine carbon sources[23], as illustrated in Fig. 2c. For example, AIR-IS $R(^{13}C/^{12}C)_{sample}$ values are accurate enough to unambiguously differentiate between C3 and C4 plant photosynthetic pathways.

With precise values of $\delta^{13}C$ assigned to our CO_2-in-air samples, traceable to VPDB, we used equation (2) to calculate $R(^{13}C/^{12}C)_{VPDB}$ from each individual spectroscopic measurement of $R(^{13}C/^{12}C)_{sample}$. A scatter plot of $R(^{13}C/^{12}C)_{VPDB}$ versus an arbitrary measurement number is shown in Fig. 3a. From the ensemble statistics of $R(^{13}C/^{12}C)_{VPDB}$ measured using samples with a variety of $\delta^{13}C$ values, we assessed long-term reproducibility associated with daily variations in the spectrum signal-to-noise ratio. The scatter in the data points plotted in Fig. 3a included variability associated with

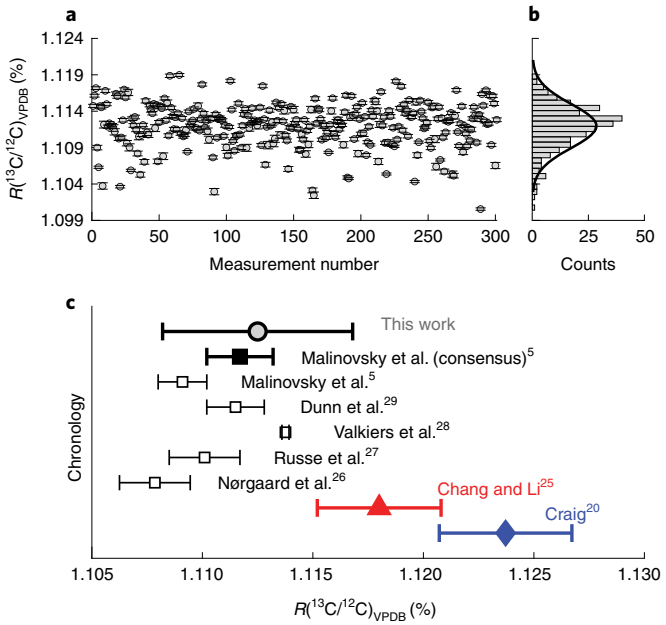

Fig. 3 | AIR-IS value of $R(^{13}C/^{12}C)_{VPDB}$. **a**, Scatter plot of all 301 unique AIR-IS measurements of $R(^{13}C/^{12}C)_{VPDB}$, along with error bars showing a relative precision of ~0.2×10^{-3}. **b**, Histogram of values fitted to a normal distribution (black line), with a mean value of $R(^{13}C/^{12}C)_{VPDB}=0.011125$. **c**, Comparison of literature values for $R(^{13}C/^{12}C)_{VPDB}$[5,20,24–29], including this work. Error bars show the combined standard uncertainty.

spectroscopic interferences, as well as potential optical interference effects (for example, spurious etalons) and daily variations in laser power and linewidth that slightly affected the optical cavity throughput and scan speed. The data were fitted to a normal distribution function (Fig. 3b) with a mean value of $R(^{13}C/^{12}C)_{VPDB}=0.011125$ and a standard error of the mean of 1.7×10^{-6}. Therefore, our Type A evaluation of the long-term reproducibility gave a relative standard uncertainty of 0.15×10^{-3}.

In addition to long-term reproducibility in a_r, we report persistent (systematic) relative standard uncertainties in $R(^{13}C/^{12}C)_{VPDB}$ for the transition intensities, cavity ring-down signal digitizer non-ideality, choice of distribution function (Supplementary Section 5), IRMS value assignments and temperature in Table 1. Adding these components in quadrature gave a combined standard uncertainty in $R(^{13}C/^{12}C)_{VPDB}$ of 43×10^{-6}.

The value of $R(^{13}C/^{12}C)_{VPDB}$ inferred from the unified AIR-IS and IRMS approach reported here is plotted as a grey circle at the top of Fig. 3c and labelled 'This work'. The error bar illustrates the combined standard uncertainty in our measurement, dominated by the uncertainty in the $^{13}C^{16}O_2$ transition intensities. For comparison, several literature values are also plotted in Fig. 3c. The blue diamond corresponds to the most widely cited value of $^{13}R_{VPDB}=0.0112372$ (standard uncertainty, 30×10^{-6}), measured by calibrated mass spectrometry of the original PeeDee Belemnite sample performed by Craig in 1957 (ref. [20]). More recently, in a 2010 technical report[24], the International Union of Pure and Applied Chemistry (IUPAC) recommended a value of $R(^{13}C/^{12}C)_{VPDB}=0.011180$ (standard uncertainty, 14×10^{-6}) based on mass spectrometry measurements by Chang and Li in 1990 (red triangle)[25]. Additional experiments performed over the last 20 years[5,26–29] (open black squares) collectively allude to an even lower absolute value of $R(^{13}C/^{12}C)_{VPDB}=0.011117$ (standard uncertainty, 15×10^{-6}) shown as the black square[5], with those literature values deviating by more than −14‰ from Craig[20].

The AIR-IS result is in good agreement with the 2019 recommendation of Malinovsky et al.[5], suggesting from that a re-evaluation

Table 1 | Uncertainty budget for $R(^{13}C/^{12}C)_{VPDB}$

Symbol	Value ($\times10^{-3}$)	Notes
u_{636}	3.80	Line intensity, $^{13}C^{16}O_2$
u_{626}	0.60	Line intensity, $^{12}C^{16}O_2$
u_{ADC}	0.60	Digitizer non-ideality
u_f	0.16	Choice of distribution function
u_{a_r}	0.15	Standard error in a_r
u_{IRMS}	0.06	IRMS $\delta^{13}C$ value assignments
u_T	0.04	Temperature dependence of S

Summary of individual relative standard uncertainties (u) comprising the combined standard uncertainty for $R(^{13}C/^{12}C)_{VPDB}$ of 43×10^{-6}

of the internationally accepted value of $R(^{13}C/^{12}C)_{VPDB}$ is appropriate. Recently, Skrzypek and Dunn[30] highlighted an immediate motivation for the adoption of an SI-traceable consensus value of $R(^{13}C/^{12}C)_{VPDB}$. They report that three different reference values are currently in use by commercial optical stable carbon isotope analysers, resulting in potential differences between the calibrated analyser δ values of ~0.1‰. Therefore, the addition of our independent AIR-IS value to the VPDB discussion will aid in establishing consistency and traceability in stable carbon isotope analysis.

By directly interrogating highly homogeneous gas-phase samples of CO_2 in air, AIR-IS avoids biases common to the general practise of CO_2 extraction from a VPDB-traceable carbonate. Furthermore, AIR-IS also eliminates the need for O-isotope calibrations, potentially allowing the technique to accurately quantify $R(^{13}C/^{12}C)_{sample}$ values even in the event of anomalous oxygen isotopic compositions. For example, careful attention must be paid to ^{17}O corrections when analysing CO_2 samples with oxygen from different sources using mass spectrometry (for example, samples originating from reactions with ^{17}O-enriched stratospheric ozone)[24]. Oxygen isotope anomalies are also observed in extraterrestrial samples and may explain early Solar System evolution[31]. Specifically, the stable carbon isotopic composition of meteorites with potentially anomalous oxygen compositions reveal ^{13}C enrichment in the organic molecules carried to early Earth[32]. These O-isotope anomalies—unless known a priori—present a unique challenge for accurate mass spectrometry where oxygen corrections are explicitly required[24,31].

The AIR-IS methodology reported here is suitable for the possible optical realization of various artefact-based scales, including ^{14}C, ^{18}O, ^{17}O, ^{15}N, ^{2}H and ^{34}S. For stable carbon isotope ratios, our own efforts to ascertain more accurate values for $^{13}C^{16}O_2$ transition intensities in the 2-μm-wavelength region using gravimetrically prepared, potentially isotopically enriched gas samples with traceability to the kilogram are just beginning. Accurate measurements of analogous $^{12}C^{16}O_2$ transitions could also reduce uncertainty in the $^{13}C^{16}O_2$ ab initio predictions (Supplementary Section 2). Those results are expected to reduce our relative combined standard uncertainty-associated $R(^{13}C/^{12}C)_{VPDB}$ to $\leq1\times10^{-3}$. Over time, a consensus determination of $R(^{13}C/^{12}C)_{VPDB}$ through comparisons amongst national metrology institutes and their partners could ultimately obviate the current cumbersome and time-consuming task of artefact-based scale management and long-term scale propagation. Combined with recent advances in the optical detection of ^{14}C with sensitivity below the modern mole fraction of 1.176 pmol mol^{-1} (refs. [33,34]), as well as emerging optical techniques for precision clumped isotope analysis[35], the possibility exists for finally realizing primary laser-based carbon and oxygen isotope metrology with traceability to the revised 'quantum' SI.

Online content

Any methods, additional references, Nature Research reporting summaries, source data, extended data, supplementary information, acknowledgements, peer review information; details of author contributions and competing interests; and statements of data and code availability are available at https://doi.org/10.1038/s41567-021-01226-y.

Received: 6 September 2020; Accepted: 17 March 2021;
Published online: 26 April 2021

References

1. Urey, H. C., Lowenstam, H. A., Epstein, S. & McKinney, C. R. Measurement of paleotemperatures and temperatures of the Upper Cretaceous of England, Denmark, and the Southeastern United States. *Geol. Soc. Am. Bull.* **62**, 399–416 (1951).
2. Coplen, T. B. et al. New guidelines for $\delta^{13}C$ measurements. *Anal. Chem.* **78**, 2439–2441 (2006).
3. Assonov, S. Summary and recommendations from the International Atomic Energy Agency Technical Meeting on the Development of Stable Isotope Reference Products (21–25 November 2016). *Rapid Commun. Mass Spectrom.* **32**, 827–830 (2018).
4. Phillips, W. D. The end of artefacts. *Nat. Phys.* **15**, 518 (2019).
5. Malinovsky, D., Dunn, P. J. H., Holcombe, G., Cowen, S. & Goenaga-Infante, H. Development and characterisation of new glycine certified reference materials for SI-traceable $^{13}C/^{12}C$ isotope amount ratio measurements. *J. Anal. At. Spectrom.* **34**, 147–159 (2019).
6. Kerstel, E. in *Handbook of Stable Isotope Analytical Techniques* (ed. de Groot, P. A.) 759–787 (Elsevier, 2004); https://doi.org/10.1016/B978-044451114-0/50036-3
7. Brand, W. A. & Coplen, T. B. Stable isotope deltas: tiny, yet robust signatures in nature. *Isotopes Environ. Health Stud.* **48**, 393–409 (2012).
8. Brenna, J. T., Corso, T. N., Tobias, H. J. & Caimi, R. J. High-precision continuous-flow isotope ratio mass spectrometry. *Mass Spectrom. Rev.* **16**, 227–258 (1997).
9. Flores, E., Viallon, J., Moussay, P., Griffith, D. W. T. & Wielgosz, R. I. Calibration strategies for FT-IR and other isotope ratio infrared spectrometer instruments for accurate $\delta^{13}C$ and $\delta^{18}O$ measurements of CO_2 in air. *Anal. Chem.* **89**, 3648–3655 (2017).
10. Corso, T. N. & Brenna, J. T. High-precision position-specific isotope analysis. *Proc. Natl Acad. Sci. USA* **94**, 1049–1053 (1997).
11. Webster, C. R. et al. Isotope ratios of H, C, and O in CO_2 and H_2O of the Martian atmosphere. *Science* **341**, 260–263 (2013).
12. Crosson, E. R. et al. Stable isotope ratios using cavity ring-down spectroscopy: determination of $^{13}C/^{12}C$ for carbon dioxide in human breath. *Anal. Chem.* **74**, 2003–2007 (2002).
13. Zare, R. N. et al. High-precision optical measurements of $^{13}C/^{12}C$ isotope ratios in organic compounds at natural abundance. *Proc. Natl Acad. Sci. USA* **106**, 10928–10932 (2009).
14. Long, D. A., Okumura, M., Miller, C. E. & Hodges, J. T. Frequency-stabilized cavity ring-down spectroscopy measurements of carbon dioxide isotope ratios. *Appl. Phys. B* **105**, 471–477 (2011).
15. Castrillo, A. et al. Amount-ratio determinations of water isotopologues by dual-laser absorption spectrometry. *Phys. Rev. A* **86**, 052515 (2012).
16. Kiseleva, M., Mandon, J., Persijn, S. & Harren, F. J. M. Line strength measurements and relative isotope ratio $^{13}C/^{12}C$ measurements in carbon dioxide using cavity ring down spectroscopy. *J. Quant. Spectrosc. Radiat. Transf.* **204**, 152–158 (2018).
17. Stoltmann, T., Casado, M., Daëron, M., Landais, A. & Kassi, S. Direct, precision measurements of isotopologue abundance ratios in CO_2 using molecular absorption spectroscopy: application to $\Delta^{17}O$. *Anal. Chem.* **89**, 10129–10132 (2017).
18. Kääriäinen, T., Richmond, C. A. & Manninen, A. Determining biogenic content of biogas by measuring stable isotopologues $^{12}CH_4$, $^{13}CH_4$, and CH_3D with mid-infrared direct absorption laser spectrometer. *Sensors* **18**, 496 (2018).
19. Abe, M. et al. Dual wavelength 3.2-μm source for isotope ratio measurements of $^{13}CH_4/^{12}CH_4$. *Opt. Express* **23**, 21786–21797 (2015).
20. Craig, H. Isotopic standards for carbon and oxygen and correction factors for mass-spectrometric analysis of carbon dioxide. *Geochim. Cosmochim. Acta* **12**, 133–149 (1957).
21. Assonov, S., Groening, M., Fajgelj, A., Hélie, J.-F. & Hillaire-Marcel, C. Preparation and characterisation of IAEA-603, a new primary reference material aimed at the VPDB scale realisation for $\delta^{13}C$ and $\delta^{18}O$ determination. *Rapid Commun. Mass Spectrom.* **34**, e8867 (2020).
22. Tans, P. & Zellweger, C. (eds) *18th WMO/IAEA Meeting on Carbon Dioxide, Other Greenhouse Gases and Related Tracers Measurement Techniques (GGMT-2015)* GAW Report No. 229 (WMO, 2016); https://library.wmo.int/opac/doc_num.php?explnum_id=3074
23. Coplen, T. B. & Shrestha, Y. Isotope-abundance variations and atomic weights of selected elements: 2016 (IUPAC Technical Report). *Pure Appl. Chem.* **88**, 1203–1224 (2016).
24. Brand, W. A., Assonov, S. S. & Coplen, T. B. Correction for the ^{17}O interference in $\delta(^{13}C)$ measurements when analyzing CO_2 with stable isotope mass spectrometry (IUPAC Technical Report). *Pure Appl. Chem.* **82**, 1719–1733 (2010).
25. Chang, T. L. & Li, W.-J. A calibrated measurement of the atomic weight of carbon. *Chin. Sci. Bull.* **35**, 290–296 (1990).
26. Nørgaard, J. V. et al. The International Measurement Evaluation Programme, IMEP-8: carbon and oxygen isotope ratios in CO_2. *Anal. Bioanal. Chem.* **374**, 1147–1154 (2002).
27. Russe, K., Valkiers, S. & Taylor, P. D. P. Synthetic isotope mixtures for the calibration of isotope amount ratio measurements of carbon. *Int. J. Mass. Spec.* **235**, 255–262 (2004).
28. Valkiers, S. et al. Preparation of synthetic isotope mixtures for the calibration of carbon and oxygen isotope ratio measurements (in carbon dioxide) to the SI. *Int. J. Mass. Spec.* **264**, 10–21 (2007).
29. Dunn, P. J. H., Malinovsky, D. & Goenaga-Infante, H. Calibration strategies for the determination of stable carbon absolute isotope ratios in a glycine candidate reference material by element analyser-isotope ratio mass spectrometry. *Anal. Bioanal. Chem.* **407**, 3169–3180 (2015).
30. Skrzypek, G. & Dunn, P. J. H. Absolute isotope ratios defining scales used in isotope ratio mass spectrometers and optical isotope instruments. *Rapid Commun. Mass Spectrom.* **34**, e8890 (2020).
31. Yurimoto, H. et al. in *Protostars and Planets V* (eds Reipurth, B. et al.) 849–862 (Univ. Arizona Press, 2007).
32. Furukawa, Y. et al. Extraterrestrial ribose and other sugars in primitive meteorites. *Proc. Natl Acad. Sci. USA* **116**, 24440–24445 (2019).
33. Galli, I. et al. Spectroscopic detection of radiocarbon dioxide at parts-per-quadrillion sensitivity. *Optica* **3**, 385–388 (2016).
34. Fleisher, A. J., Long, D. A., Liu, Q., Gameson, L. & Hodges, J. T. Optical measurement of radiocarbon below unity fraction modern by linear absorption spectroscopy. *J. Phys. Chem. Lett.* **8**, 4550–4556 (2017).
35. Prokhorov, I., Kluge, T. & Janssen, C. Optical clumped isotope thermometry of carbon dioxide. *Sci. Rep.* **9**, 4765 (2019).

Methods

AIR-IS. We performed frequency-agile rapid-scanning cavity ring-down spectroscopy[36] using two distributed feedback diode lasers simultaneously coupled to a single high-finesse enhancement cavity and sample cell. Long-term stability and reproducibility were achieved in part by actively stabilizing the uniform grid of optical frequencies transmitted by the enhancement cavity to a frequency-stabilized He–Ne laser[37]. The enhancement cavity and sample cell comprised two triple-coated high-reflectivity mirrors at opposite ends of a stainless steel tube. One of the mirrors was mounted to a piezo-electric transducer that was used as a slow actuator to adjust the cavity length to maintain resonance with the He–Ne laser. The optical cavity was nominally 75 cm in length, with a free spectral range of 200.07 MHz (standard uncertainty, 30 kHz).

Before introduction of CO_2-in-air samples, the sample cell was evacuated under a high vacuum for approximately 1 h and then flushed with a continuous flow of high-purity N_2 gas for approximately 2 h. The procedure effectively eliminated sample cell memory of the previous CO_2-in-air sample, as well as minimized spectroscopic interferences from previously adsorbed molecules within the gas delivery system. CO_2-in-air samples were then introduced and maintained at a constant pressure near 8 kPa (as measured by calibrated microbolometer gauges) for a total time of 2 h. After 2 h, the sample was evacuated, and the cavity was prepared to receive another sample. Temperature stabilization was enhanced using an insulating box around the AIR-IS sample cell and was monitored during spectral acquisition using calibrated platinum resistance thermometers in good thermal contact with the outside of the enhancement cavity. A comprehensive summary of the National Institute of Standards and Technology (NIST) technical approach to accurate gas metrology by cavity ring-down spectroscopy can be found in Fleurbaey et al.[38]

Digitizer linearity. Linearity of the analogue-to-digital acquisition cards was tested using synthetic exponential decay signals and a metrology-grade reference digitizer as a transfer standard[39]. The synthetic decays of 1 ms in length were constructed using an arbitrary waveform generator with 14-bit vertical resolution and a sampling rate of 128 MS s^{-1}. Their time constants spanned the relevant range for each digitizer: 26–45 µs for the 2.0 µm digitizer ($^{13}C^{16}O_2$) and 10–20 µs for the 1.6 µm digitizer ($^{12}C^{16}O_2$). Linear fits of observed time constants (τ_{obs}) versus programmed time constants (τ_{pro}) yielded a transformation function between the observed and true round-trip losses in the enhancement cavity. The linear transformations were used to estimate the relative shift in the measured integrated absorption $\delta_a = \frac{a_{obs}}{a_{pro}} - 1$ for simulated lines at both 2.0 µm and 1.6 µm. The digitizer analysis yielded the following δ_a, which were then applied to all the measured spectra: $\delta_a = 4.7 \times 10^{-3}$ for $^{13}C^{16}O_2$ at 2.0 µm and $\delta_a = -4.8 \times 10^{-3}$ for $^{12}C^{16}O_2$ at 1.6 µm. We estimated the uncertainty in δ_a to be equal to $\sqrt{2} \times 0.4 \times 10^{-3} \approx 0.6 \times 10^{-3}$ by fitting a generalized extreme value distribution function to the observed distribution in τ_{obs} over a broad range of synthetic exponential decay signals. We note that the limit in the uncertainty in δ_a is $1/(2^{\Delta+1}\sqrt{3}) \approx 0.02 \times 10^{-3}$, as calculated from the vertical resolution (Δ = 14 bits) of the arbitrary waveform generator. The measured values of δ_a estimated all the potential nonlinearities, impedance mismatches, radiofrequency back reflections, dissimilar metallic connectors and other issues associated with all electronics and cables after the photoreceivers, including the digitizer.

Gas samples and $\delta^{13}C$ value assignments. Five CO_2-in-air samples were measured by AIR-IS. The NIST Standard Reference Material 1720 Northern Continental Air with WMO/NOAA-assigned $\delta^{13}C = -8.6‰$ (cylinder number CC324315 and sample number 1720-A-25)[40,41] is mentioned in the main text. The remaining four CO_2-in-air samples, having nominal CO_2 molar fractions approximately equal to atmospheric natural abundances (~400 µmol mol^{-1}), were prepared at the NIST. Briefly, the preparation involved mixing (diluting) isotopically distinct pure CO_2 (>99.996%) samples with a balance of synthetic air (N_2, 78.1%; O_2, 20.89%; CO_2, <0.3 µmol mol^{-1}; N_2O, <0.2 nmol mol^{-1}) using gravimetric and volumetric standard preparation methods for compressed gas mixtures[40,42].

The VPDB-CO_2 $\delta^{13}C$ and $\delta^{18}O$ value assignments of these four samples were made at the NIST on the parent CO_2 by dual-inlet isotope ratio mass spectrometry (DI-IRMS)[43]. The NIST VPDB-CO_2 scale realization was achieved by using NIST pure CO_2 reference materials 8562, 8563 and 8564 (ref. [44]). A summary of NIST DI-IRMS results and related gas sample information is provided in Supplementary Table 4. Importantly, the uncertainty of 0.06‰ associated with the NIST IRMS value assignments had a minimal impact on the absolute isotope ratio $R(^{13}C/^{12}C)_{VPDB}$ estimated in this work. Further details regarding the assignment uncertainties of the IRMS value can be found in Srivastava and Verkouteren[43] and Supplementary Section 4.

Isotope ratio notation and nomenclature. Here we use notation for isotope ratios recommended by the Commission on Isotopic Abundances and Atomic Weights of the IUPAC[45].

Quantum chemistry calculations. Rotational–vibrational transition intensities were calculated for $^{13}C^{16}O_2$ using an updated ab initio DMS and semi-empirical PES. Here we improved upon the ab initio DMS of Polyansky et al.[46] by increasing the number of ab initio data points by 50% (3,000 total points). Also, the semi-empirical PES of Huang et al.[47], previously used by Polyansky et al.[46] without modification, was fitted to known CO_2 energy levels using the DVR3D programme[48] resulting in a standard deviation of 0.02 cm^{-1}. Analogous quantum chemistry methods recently applied to water showed that both an increased number of ab initio DMS data points[49] and an accurate semi-empirical PES[50] improve the accuracy of the predicted transition intensities.

For our denser grid of ab initio points, we applied the same level of quantum chemistry theory as Polyansky et al.[46] An all-electron multireference configuration interaction calculation with the aug-cc-pwCVQZ basis set, inclusive of relativistic corrections, was determined from separately fitted one-electron mass–velocity–Darwin terms. The Molpro package[51] was used for the calculations, and the wavefunctions—required to predict the transition intensities—were numerically solved from the rotational–vibrational Schrödinger equation using the DVR3D programme[48].

To evaluate the uncertainty in the predicted $^{13}C^{16}O_2$ transition intensities, we also calculated the transition intensities for $^{12}C^{16}O_2$ and compared with highly accurate experiments[38,52–54]. For ground-state rotational quantum numbers of $J'' = 12$ and $J'' = 18$, we find that for five near-infrared vibrational bands of $^{12}C^{16}O_2$, the standard deviation of a uniform distribution chosen to represent the experimental measurements relative to the predictions of our updated ab initio DMS is equal to 3.8×10^{-3}. This value, listed in Table 1 of the main text as the uncertainty in the $^{13}C^{16}O_2$ transition intensities, is consistent with upper-bound estimates from quantum chemistry methods[46,55]. Further details, including numerical results from the updated ab initio DMS and their comparison with the experimental literature, can be found in Supplementary Sections 1 and 2.

Data availability

Source data are provided with this paper, and are additionally available at https://doi.org/10.18434/mds2-2369. All other data that support the plots within this paper and other findings of this study are available from the corresponding author upon reasonable request.

References

36. Truong, G. W. et al. Frequency-agile, rapid scanning spectroscopy. *Nat. Photon.* **7**, 532–534 (2013).
37. Hodges, J. T., Layer, H. P., Miller, W. W. & Scace, G. Frequency-stabilized single-mode cavity ring-down apparatus for high-resolution absorption spectroscopy. *Rev. Sci. Instrum.* **75**, 849–863 (2004).
38. Fleurbaey, H., Yi, H., Adkins, E. M., Fleisher, A. J. & Hodges, J. T. Cavity ring-down spectroscopy of CO_2 near $\lambda = 2.06$ µm: accurate transition intensities for the Orbiting Carbon Observatory-2 (OCO-2) "strong band". *J. Quant. Spectrosc. Radiat. Transf.* **252**, 107104 (2020).
39. Fleisher, A. J. et al. Twenty-five-fold reduction in measurement uncertainty for a molecular line intensity. *Phys. Rev. Lett.* **123**, 043001 (2019).
40. Rhoderick, G. C. et al. Development of a Northern Continental Air standard reference material. *Anal. Chem.* **88**, 3376–3385 (2016).
41. *NOAA Central Calibration Laboratory Reference Gas Calibration Results for NIST Standard Reference Material 1720 Northern Continental Air Serial Number CC324315* (accessed 17 February 2021); https://www.esrl.noaa.gov/gmd/ccl/refgas.html
42. Milton, M. J. T., Guenther, F., Miller, W. R. & Brown, A. S. Validation of the gravimetric values and uncertainties of independently prepared primary standard gas mixtures. *Metrologia* **43**, L7–L10 (2006).
43. Srivastava, A. & Verkouteren, R. M. Metrology for stable isotope reference materials: $^{13}C/^{12}C$ and $^{18}O/^{16}O$ isotope ratio value assignment of pure carbon dioxide gas samples on the Vienna PeeDee Belemnite-CO_2 scale using dual-inlet mass spectrometry. *Anal. Bioanal. Chem.* **410**, 4153–4163 (2018).
44. Verkouteren, R. M. & Klinedinst, D. B. *Value Assignment and Uncertainty Estimation of Selected Light Stable Isotope Reference Materials: RMs 8543–8545, RMs 8562–8564, and RM 8566* NIST Special Publication 260-149 (NIST, 2004); https://www.nist.gov/document-10350
45. Coplen, T. B. Guidelines and recommended terms for expression of stable-isotope-ratio and gas-ratio measurement results. *Rapid Commun. Mass Spectrom.* **25**, 2538–2560 (2011).
46. Polyansky, O. L. et al. High-accuracy CO_2 line intensities determined from theory and experiment. *Phys. Rev. Lett.* **114**, 243001 (2015).
47. Huang, X., Schwenke, D. W., Tashkun, S. A. & Lee, T. J. An isotopic-independent highly accurate potential energy surface for CO_2 isotopologues and an initial $^{12}C^{16}O_2$ infrared line list. *J. Chem. Phys.* **136**, 124311 (2012).
48. Tennyson, J. et al. DVR3D: a program suite for the calculation of rotation–vibration spectra of triatomic molecules. *Comput. Phys. Commun.* **163**, 85–116 (2004).

49. Conway, E. K., Kyuberis, A. A., Polyansky, O. L., Tennyson, J. & Zobov, N. F. A highly accurate ab initio dipole moment surface for the ground electronic state of water vapour for spectra extending into the ultraviolet. *J. Chem. Phys.* **149**, 084307 (2018).
50. Mizus, I. I. et al. High-accuracy water potential energy surface for the calculation of infrared spectra. *Phil. Trans. R. Soc. A* **376**, 20170149 (2018).
51. Werner, H.-J., Knowles, P. J., Knizia, G., Manby, F. R. & Schütz, M. Molpro: a general-purpose quantum chemistry program package. *Wiley Interdiscip. Rev. Comput. Mol. Sci.* **2**, 242–253 (2012).
52. Long, D. A. et al. High-accuracy near-infrared carbon dioxide intensity measurements to support remote sensing. *Geophys. Res. Lett.* **47**, e2019GL086344 (2020).
53. Wübbeler, G., Víquez, G. J. P., Jousten, K., Werhahn, O. & Elster, C. Comparison and assessment of procedures for calculating the R(12) line strength of the $\nu_1+2\nu_2+\nu_3$ band of CO_2. *J. Chem. Phys.* **135**, 204304 (2011).
54. Yi, H., Liu, Q., Gameson, L., Fleisher, A. J. & Hodges, J. T. High-accuracy $^{12}C^{16}O_2$ line intensities in the 2 μm wavelength region measured by frequency-stabilized cavity ring-down spectroscopy. *J. Quant. Spectrosc. Radiat. Transf.* **206**, 367–377 (2018).
55. Lodi, L. & Tennyson, J. Line lists for $H_2{}^{18}O$ and $H_2{}^{17}O$ based on empirical line positions and ab initio intensities. *J. Quant. Spectrosc. Radiat. Transf.* **113**, 850–858 (2012).

Acknowledgements

We acknowledge M. E. Kelley and W. R. Miller Jr, (NIST) for preparing several CO_2-in-air gas samples. Funding was provided by the NIST Greenhouse Gas and Climate Science Program. O.L.P. acknowledges partial support from the Quantum Pascal project 18SIB04, which received funding from the EMPIR programme co-financed by the Participating States and the European Union's Horizon 2020 research and innovations programme. N.F.Z. acknowledges State project 0035-2019-0016.

Author contributions

A.J.F. assisted with the experimental design, assembly and characterization; performed data analysis; and wrote the Letter. H.Y. assembled optical instrumentation and performed spectroscopy on the CO_2-in-air samples. A.S. performed isotope ratio mass spectrometry on the parent CO_2 samples. O.L.P. and N.F.Z. performed quantum chemistry calculations of CO_2 transition intensities. J.T.H. conceived the experimental design and assisted with instrumentation, data analysis and reduction. All the authors contributed to the final written Letter.

Competing interests

The authors declare no competing interests.

Additional information

Supplementary information The online version contains supplementary material available at https://doi.org/10.1038/s41567-021-01226-y.

Correspondence and requests for materials should be addressed to A.J.F.

Peer review information *Nature Physics* thanks the anonymous reviewers for their contribution to the peer review of this work.

Reprints and permissions information is available at www.nature.com/reprints.